any of these adversities would develop some of the physiological disorders such as leaf reddening or senescence, square and boll shedding, parawilt or suddenwilt, bad opening of bolls, etc. Quite often these disorders are reported in farmers' fields. This understanding of temporal and spatial distribution of fruiting forms in *Bt* and N*Bt* hybrids might help in evolving efficient physical, chemical or biological management strategies to overcome the above disorders.

1. Mohan, K. S. and Manjunath, T. M., *Bt* cotton – India's first transgenic crop. *J. Plant Physiol.*, 2002, **29**, 225–236.
2. Ramasundaram, P., The performance of *Bt* cotton hybrids in India. *ICAC Rec.*, 2005, **23**, 17–18.
3. Guinn, G., Fruiting of cotton. III. Nutritional stress and cutout. *Crop Sci.*, 1985, **25**, 981–985.
4. Stewart, S. D. and Sterling, W. L., Susceptibility of cotton fruiting forms to insects, boll rot and physical stress. *J. Econ. Entomol.*, 1989, **82**, 593–598.
5. Constable, G. A., Mapping the production and survival of fruit on field grown cotton. *Agron. J.*, 1991, **83**, 374–378.
6. Guinn, G., Abscission of cotton floral buds and bolls as influenced by factors affecting photosynthesis and respiration. *Crop Sci.*, 1974, **14**, 291–293.
7. Hebbar, K. B., Perumal, N. K. and Khadi, B. M., Photosynthesis and plant growth response of transgenic *Bt* cotton (*Gossypium hirsutum* L.) hybrids under field condition. *Photosynthetica*, 2007, **45**, 254–258.
8. Bhatt, J. G., In *Cotton Physiology* (eds Sundaram, D. V. and Rao, S. B. P.), Cotton Monograph Series, Indian Society for Cotton Improvement, Mumbai, 1996, pp. 26–37.

Received 19 October 2006; revised accepted 4 June 2007

Self-rotation of an assembly of two or more cylindrical objects in optical tweezers: A simple approach for realization of optically driven micromotors

Samarendra K. Mohanty, Pradeep K. Gupta and Ravi S. Verma*

Biomedical Applications Section, Raja Ramanna Centre for Advanced Technology, Indore 452 013, India

We show that an assembly of two or more cylindrical objects rotates by itself when trapped in conventional optical tweezers. The rotational speed and direction of rotation were observed to depend on the asymmetry of the structure, and for a given structure the speed was found to increase linearly with increase in the trapping beam power. A ray optic model was also developed for the assembly of rods. Its predictions on the direction of rotation and the optical torque on the assembly were in qualitative agreement with the experimental observations. Such an assembly of rods may provide a convenient and dynamically reconfigurable approach for optically driven micromotors.

Keywords: Microfluidics, micromotors, optical trapping, optical tweezers.

THERE exists considerable interest on the development of optically driven micromotors as these could be driven remotely by laser beams and thus could play an important role in various microfluidic applications. A variety of methods have therefore been developed for rotation of optically trapped objects[1–5]. One approach actively pursued towards this objective is to fabricate structures that experience windmill-type torque by transfer of linear momentum from the trapping beam and thus rotate[6,7]. However, fabrication of such special structures is complicated and costly, and may limit the use of this approach. We show in this communication that an assembly of two or more cylindrical objects provides a convenient and dynamically reconfigurable approach for optically driven micromotors. Further, the individual rods can be transported through narrow channels (with width smaller than the size of the micromotor), either by microfluidic flow or by laser tweezers to the desired location where they can be assembled to construct micromotors and dismantled after use. We also describe a ray optic model for the assembly, which accurately predicts the direction of rotation as well as dependence of the torque on the asymmetry of the structure.

We used a conventional inverted optical tweezers setup for studies on the dynamical behaviour of an assembly of cylindrical rods when subjected to a trapping beam. The output of a 1064 nm, TEM_{00} mode, cw Nd : YAG laser (Solid State Laser Division, Raja Ramanna Centre for Advanced Technology, Indore, India) was coupled to a 100X/1.3 microscope objective (Carl Zeiss GmbH, Jena, Germany) and used as the trapping beam. The sequence of digitized images, acquired using a CCD camera and frame-grabber, was used for studying the dynamical behaviour of the assemblies of micro-rods. To prevent the backscattered laser light from reaching the CCD detector, an IR cut-off filter was used. The laser beam power was measured at the back aperture of the microscope objective using a power meter (Coherent Inc., USA). The trapping beam power at the sample plane was estimated using the transmission factor of the objective (57%) that was determined using the dual objective technique described by Misawa *et al.*[8]. The glass rods (Nippon Electric Glass Co Ltd, Japan) used in the study had diameter of ~5 μm and lengths varying from 10 to 30 μm.

It is known[9–11] that when placed in a point optical tweezers, a cylindrical rod gets aligned along the axis of

*For correspondence. (e-mail: rsverma@cat.ernet.in)

the laser beam that is normal to the plane of the microscope stage. The behaviour of an assembly of two similar rods when trapped simultaneously in the same trapping beam (120 mW) is shown in Figure 1. As can be seen in Figure 1, one of the two rods (marked by arrow) gets oriented along the axis of the laser beam and the other rod remains almost horizontal and rotates in the clockwise direction about the rod aligned along the laser axis. Figure 2 shows the variation of rotational speed of this rod assembly as a function of the trapping beam power. The rotational speed was observed to increase linearly with a slope of ~1.50 rpm/mW.

It is pertinent to note that the assembly of two cylindrical rods placed in the same trap beam, shown schematically in Figure 3 *a*, results in a structure that resembles one of the four arms of the structure investigated in detail by Higurasi *et al.*[7] and Gauthier[9]. In conformity with their analysis, the origin of the torque in the present assembly appears to arise due to asymmetry of the structure (the two long sides of the horizontally placed cylinder not being symmetrical with respect to the rod trapped vertically along the laser beam). An exact modelling of the torques induced by the trapping beam on the assembly of two cylindrical objects will be complicated. In order to keep the simulation simple, we ignored the effect of the vertically oriented rod on the propagation of the trap beam and used the theoretical model developed earlier by Gauthier *et al.*[9–11] to estimate the torque on the horizontal cylindrical rod as a function of its position with respect to the trap beam focal point. Following Gauthier[9], the z-axis directed TEM_{00} unpolarized Hermite–Gaussian laser beam can be treated as a stream of photons, which are made incident on the cylindrical object. As the photon undergoes reflection and refraction at the point of incidence, there is a transfer of momentum. If (l_i, m_i, n_i), (l_r, m_r, n_r) and (l_t, m_t, n_t) are the direction cosines for the incident, reflected and refracted rays, the momentum transferred to the object from the reflected photon is:

$$d\vec{P}_r = \frac{hn_1}{\lambda}\{(l_i - l_r)\hat{x} + (m_i - m_r)\hat{y} + (n_i - n_r)\hat{z}\}, \quad (1)$$

and from refracted photon is:

$$d\vec{P}_t = \frac{hn_1}{\lambda}\{(l_i - n_{rel}l_t)\hat{x} + (m_i - n_{rel}m_t)\hat{y} + (n_i - n_{rel}n_t)\hat{z}\}. \quad (2)$$

Here λ is the wavelength of the trapping laser beam in vacuum, h is the Plank constant and $n_{rel} = n_2/n_1$, where n_2 is the index of refraction of the object and n_1 that of the ambient medium. Thus the total force exerted by all the photons reflected or refracted at the interface of the cylinder and ambient medium can be written as:

$$\vec{F} = \sum d\vec{F}_i = \sum N_i\{R_{avg}d\vec{P}_r + (1 - R_{avg})d\vec{P}_t\}. \quad (3)$$

N_i is the number of photons per second incident at the point centred on the ith elemental area of the rod, and R_{avg} is the average of the reflection coefficients (calculated using Fresnel formula) for the two orthogonal polarizations (TE and TM) of the laser beam. The summation is over the entire elemental area of the rod. It is known that a cylinder placed in a laser trap localizes such that its overlap with the high-intensity region is maximized. Therefore, for the two-rod assembly, one of the rods aligns along the trap beam and the other will try to orient about this rod such that it also maximizes overlap with the region of high intensity. The experimental results (Figure 1) suggest that the second rod is almost horizontal. Therefore, to keep simulation tractable, we assumed the other rod to be exactly horizontal. The torque on the horizontal rod as a function of its position in the XY-plane can be calculated as:

$$\vec{\tau} = \sum(\vec{r}_i \times d\vec{F}_i). \quad (4)$$

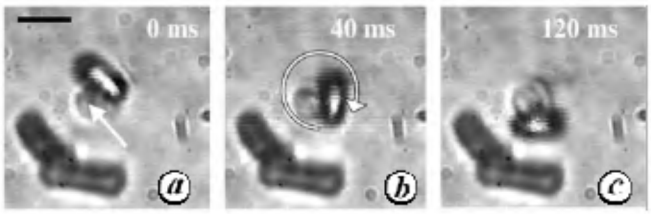

Figure 1. Digitized time-lapse video images showing dynamics of an assembly of two cylindrical rods of nearly the same length when trapped in optical tweezers. One of these (marked by arrow) gets oriented with its axis aligned along the axis of the laser beam and the other remains almost horizontal and rotates about the other rod (*a* to *c*). Direction of rotation is shown by curved arrow. Scale bar: 10 μm.

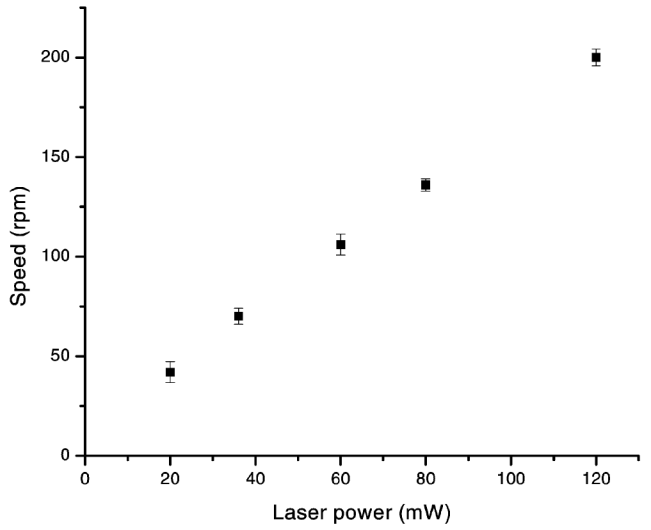

Figure 2. Variation of rotational speed of the two-rod assembly as a function of trapping beam power. Symbols represent the mean of five measurements and error bars show standard deviation about the mean.

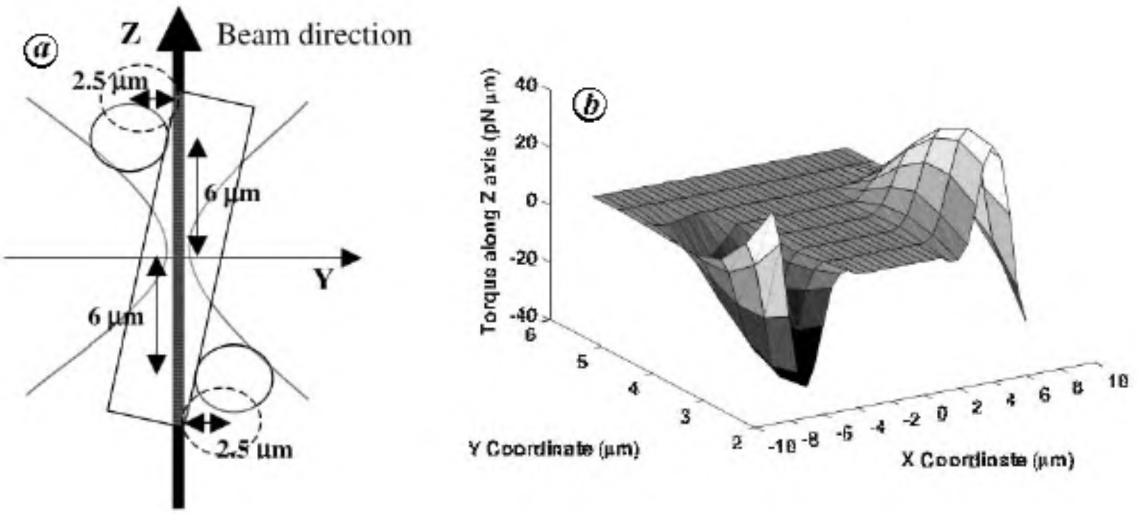

Figure 3. ***a***, Schematic of side view of the cross-section of the two-rod assembly. Solid circles show the vertical position of the horizontally placed rod where the whole width of the rod interacts with the beam. Dashed circles show the closest position of the horizontal rod in the *Y*-direction. ***b***, Estimates for torque on the horizontally placed rod (L = 15 µm), when the axis of the rod was 4 µm above the plane of focus. Trap beam power was taken to be 120 mW. Torque was calculated only for the positive displacement (from 2.5 to 6 µm in the *Y*-direction) of the centre of the cylinder with respect to the beam.

Here $\vec{r}_i$ is the radial distance of the ith element from the origin (centre of the beam waist) and dF_i is the force on this element. Since at $Z = 0$, the rod will have negligible interaction with the trap beam, it has to be located at a plane above or below $Z = 0$. As we move vertically up/down in the Z-plane, the interaction of the rod with the beam emerging out of the vertically trapped rod increases. A simple calculation shows that the whole width of the rod in transverse direction interacts with the trap beam at a plane located at ~±6 µm from the focal plane. This is shown in Figure 3 *a* by solid circles. However, the intensity of the trap beam decreases rapidly as we move away from the focal plane. The stable trap position for the rod is, therefore, expected to be in the region lying between planes $Z = 0$ µm and $Z = 6$ µm. Our experimental results suggest that this was ~± 4 µm. We therefore calculated the torque acting on a horizontally placed rod (radius: 2.5 µm and length: 15 µm) at a plane 4 µm above the plane of focus. For a laser beam power of 120 mW, the results are shown in Figure 3 *b*. Since the horizontal rod cannot come closer than 2.5 µm (shown by dashed circles in Figure 3 *a*) in the *Y*-direction due to the presence of the vertical rod, the lower *Y*-limit of calculations was kept at 2.5 µm. A perusal of Figure 3 *b* shows that the torque on the rod is zero when it is placed symmetrically with respect to the centre of the beam waist and increases in magnitude as the asymmetry of the assembly increases by displacement of the rod in the *X*-direction on either side. Further, it is important to note that the sign of the torque changes in (+) and (–) *X*-quadrants, suggesting that the displacement of the horizontal rod in (+) or (–) *X*-direction from the beam waist determines the sense of rotation. This is consistent with the experimental results presented in Figure 1.

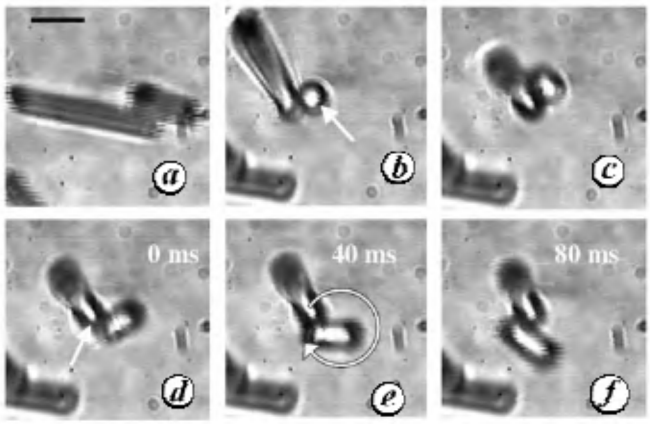

Figure 4. Digitized time-lapse video images showing dynamics of an assembly of two cylindrical rods with the same radius but unequal lengths when trapped in optical tweezers. The longer rod orients vertically (***a–c***) and the smaller rod revolves (***d–f***) around the longer trapped rod (marked by arrow). Scale bar: 10 µm.

The dynamics was even more interesting when two rods of unequal lengths were trapped. The behaviour of an assembly of two unequal rods trapped simultaneously in the same trapping beam (80 mW) is shown in Figure 4 *a–f*. In this case, it was observed that the bigger rod was always aligned along the laser beam axis even if at first the smaller rod was so aligned. To understand this, we would like to point out that in case of a single trapped rod, the equilibrium is obtained only when the rod is aligned along the trap beam. In such an orientation, the effective potential energy of the rod inside the trap is minimized as it ensures maximum overlap of the rod with the trap beam[10]. Using the same arguments, we believe that in case of a two-rod assembly, aligning of the longer rod with the trap beam axis ensures minimization of potential

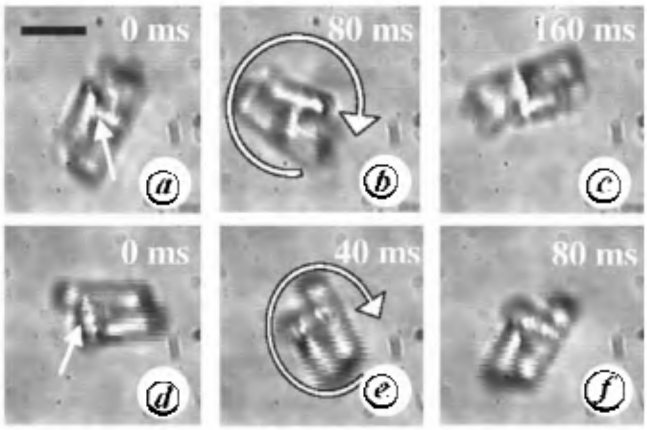

Figure 5. Time-lapse digitized video images showing dynamics of an assembly of three cylindrical objects when optically tweezed by the same trapping beam (120 mW). ***a–c***, Rotation where the two horizontally oriented rods were placed asymmetrically with respect to the vertically trapped rod. ***d–f***, The case when one of their ends is in contact with the vertical rod. The trapped rod is marked by straight arrow and the direction of rotation is shown by curved arrow. Scale bar: 10 μm.

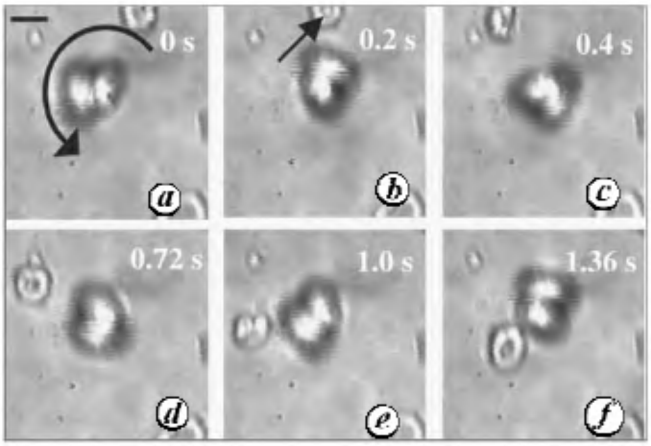

Figure 6. Time-lapse digitized video images showing fluid flow induced by the optically driven two-rod assembly. Fluid flow is monitored by tracking of a tracer object (RBC, marked by arrow). Curved arrow shows the direction of rotation. Scale bar: 10 μm.

energy of the rod assembly inside the trap beam. In Figure 4 *a–c*, one can see the bigger rod displacing the smaller one (marked by arrow) to get oriented along the laser axis. The smaller rod then revolves (Figure 4 *d–f*) around the longer trapped rod (marked by arrow).

An assembly of more than two cylindrical rods shows even richer dynamics. When two additional rods were trapped near an already trapped and aligned rod (marked by arrow in panel Figure 5 *a*), these were found to rotate. In addition to the trap beam power, the rotation speed was found to depend on the arrangement of the trapped rods. Figure 5 *a–c* shows the rotation of a three-rod assembly, where the two horizontally oriented rods were placed asymmetrically with respect to the vertically trapped rod. When the horizontal rods were placed with one of their ends in contact with the vertical rod (marked by arrow in Figure 5 *d*), the structure rotated with higher rotational speeds (Figure 5 *d–f*), because increased asymmetry of the structure led to higher torques. The optically driven two-rod assembly was used for controlling microfluidic flow. Rotation of the rod-motor resulted into controlled fluid flow. Figure 6 shows fluid flow induced by the optically driven two-rod assembly. The rotating rod-assembly was held at ~10 μm from the bottom coverslip. The direction of flow was controlled by controlling the direction of rotation of the motor and flow rate by controlling the speed of rotation, which was in turn controlled by a change in power of the trapping beam. Movement of a tracer object (marked by arrow), such as a red blood cell (RBC), was used to monitor the flow direction and rate. The drag forces induced by the rotating assembly caused the tracer object in the surrounding medium to follow a circular path. From the movement of the tracer object (RBC, assuming to be a disk of diameter ~8 μm and width ~3 μm), the fluid flow rate induced by rotation of a two-rod assembly at a trapping power of 120 mW was found to be ~5 nl/h.

To conclude, we have shown that an assembly of two or more cylindrical rods rotates when trapped by optical tweezers. Such an assembly of rods may provide a convenient and dynamically reconfigurable approach for optically driven micromotors.

1. He, H., Friese, M. E. J., Heckenberg, N. R. and Rubinsztein-Dunlop, H., Direct observation of transfer of angular momentum to absorptive particles from a laser beam with a phase singularity. *Phys. Rev. Lett.*, 1995, **75**, 826–829.
2. Paterson, L., MacDonald, M. P., Arit, J., Sibbett, W., Bryant, P. E. and Dholakia, K., Controlled rotation of optically trapped microscopic particles. *Science*, 2001, **292**, 912–914.
3. Dasgupta, R., Mohanty, S. K. and Gupta, P. K., Controlled rotation of biological, microscopic objects using optical line tweezers. *Biotechnol. Lett.*, 2003, **25**, 1625–1628.
4. Friese, M. E. J., Nieminen, T. A., Hewckenberg, N. R. and Rubinsztein-Dunlop, H., Optical alignment and spinning of laser-trapped microscopic particles. *Nature*, 1998, **394**, 348–350.
5. Dasgupta, R. and Gupta, P. K., Rotation of transparent, nonbirefringent objects by transfer of the spin angular momentum of light. *Opt. Lett.*, 2005, **30**, 394–396.
6. Galajda, P. and Ormos, P., Complex micromachines produced and driven by light. *Appl. Phys. Lett.*, 2001, **78**, 249–251.
7. Higurasi, E., Ukita, H., Tanaka, H. and Ohguchi, O., Optically induced rotation of anisotropic micro-objects fabricated by surface micromachining. *Appl. Phys. Lett.*, 1994, **64**, 2209–2210.
8. Misawa, H., Koshioka, M., Sasak, K., Kitamura, N. and Masuhara, H., Three dimensional optical trapping and laser ablation of a single polymer latex in water. *J. Appl. Phys.*, 1991, **70**, 3829–3836.
9. Gauthier, R. C., Optical trapping: A tool to assist optical machining. *Opt. Laser. Technol.*, 1997, **29**, 389–399.
10. Gauthier, R. C., Theoretical investigation of the optical trapping force and torque on cylindrical micro-objects. *J. Opt. Soc. Am. B*, 1997, **14**, 3323–3333.
11. Gauthier, R. C., Ashman, M. and Grover, C. P., Experimental confirmation of the optical-trapping properties of cylindrical objects. *Appl. Opt.*, 1999, **38**, 4861–4868.

ACKNOWLEDGEMENTS. We thank Mr R. Dasgupta (BMAS, RRCAT, Indore) for making available the glass rods, and Ms Khyati Dave for help during the experiments.

Received 9 September 2006; revised accepted 16 March 2007